

The Scale Invariant Scotogenic Model: Dark Matter and the Scalar Sector

Rachik Soualah^{1,2*} and Amine Ahriche^{1,2†}

¹*Department of Applied Physics and Astronomy, University of Sharjah, UAE. and*

²*The International Center for Theoretical Physics
(ICTP)- Strada Costiera, 11, I - 34151 Trieste Italy.*

Abstract

In this paper, we investigate the mutual impact between the dark matter (DM) requirements and the scalar sector in the scale invariant (SI) scotogenic model. The model is motivated by the neutrino mass and DM within a classically SI framework. It is a SI generalization of the scotogenic model, where the standard model (SM) is extended by a real singlet, an inert scalar doublet and three Majorana singlet fermions, where the lightest one (N_1) could play the DM candidate role. In addition to the annihilation channels $N_1 N_1 \rightarrow \ell_\alpha \ell_\beta, \nu_\alpha \bar{\nu}_\beta$, the DM can be annihilated via few s-channel processes into SM particles, that are mediated by the Higgs/dilaton. This allows the new Yukawa interactions, that are responsible for neutrino mass generation, to take small values and therefore avoid the mass degeneracy between the CP-even and CP-odd inert scalars unlike the case of the minimal scotogenic model. In contrast to many Majorana DM models, the DM in the SI-scotogenic model couples to the quarks at tree-level, and hence the constraint from the direct detection experiments is very important on the space parameter. The aim of this work is to investigate the correlation between the DM requirements and the scalar sector in this model.

* rsoualah@sharjah.ac.ae, rsoualah@cern.ch

† ahriche@sharjah.ac.ae, amine.ahriche@cern.ch

I. INTRODUCTION

The discovery of the Higgs boson on July 2012 provided a well established explanation of the mass origin of the fermions and gauge bosons of the standard model (SM). However, despite this great breakthrough, many questions are still open, such as the origin of neutrino mass and its smallness, the dark matter (DM) nature, that appears necessary at the galactic scale. In addition to these unanswered questions, it is so puzzling that most of the mass-dimension parameters in the SM are of the order of $\mathcal{O}(100)$ GeV. Therefore, we still have too much to learn about the mechanism(s) of masses at the Universe. In regards to this open issue, recent works have studied several extensions of the SM that possess a scale-invariance (SI) symmetry, where the electroweak symmetry breaking (EWSB) occurs as a quantum effect via the radiative symmetry breaking a la Coleman-Weinberg [1]. These models are phenomenologically rich, and generally predict new TeV mass particles, that could be within the reach of the LHC.

A popular explanation of the smallness of the neutrino mass is provided by the so-called seesaw mechanism [2], where a hierarchy between the charged leptons and neutrinos masses emerges due to the hierarchy between the electroweak (EW) scale and the heavy singlet Majorana fermion mass, that are added to the SM. The new high scale (Majorana fermion mass) makes this scenario impossible to be probed at the current and near future high energy colliders. Another attractive approach is that the radiative neutrino mass is massless at tree level and acquire a naturally small Majorana mass term at the loop level: one-loop [3, 4], two loops [5–9], three loops [10–22], and four loops [23]. Some of these models address the DM problem where a massive Majorana DM with a mass range from GeV to TeV can play an important role as a DM candidate [3, 11, 12, 14], in addition to the neutrino oscillation data. Furthermore, these models predict interesting signatures at current/future collider experiments [24–26] (for a review, see [27]).

Extending some of the ν -DM motivated models by incorporating the SI symmetry, makes the model phenomenology modified and richer [28]. Indeed, one can emphasize that by considering the SI symmetry the issues of ESWB, neutrino mass and DM are solved all together at the EW scale. For example, the models in [29] and [10] are SI generalizations of a one-loop (scotogenic [30]) and a three-loop (KNT [11]) model, where the lightest Majorana fermion plays the DM role. In addition to the DM annihilation channel $N_1 N_1 \rightarrow \ell_\alpha \ell_\beta, \nu_\alpha \bar{\nu}_\beta$ in the scotogenic model (and similarly with the SI-KNT model [10]), other channels such as $N_1 N_1 \rightarrow h_i h_k, VV, q\bar{q}$, are possible to take place due to the DM coupling with the Higgs/dilaton in the SI extensions. Here, $V = W, Z$ are the SM gauge bosons, and h_i could be the Higgs H and/or the the lighter CP-even eigenstate D , that is called the dilaton in the SI models. It is strictly massless at tree-level and acquires its mass via the loop

corrections. In the non SI models (for example [11] and [30]), for a given DM mass M_1 , the relic density dictates the values of the new Yukawa couplings ($g_{i\alpha}$) that couple the left-handed lepton doublets (or the charged right-handed leptons in the case of KNT model) and the inert doublet (charged singlet) scalar. This makes the values of these couplings ($g_{i\alpha}$) too constrained since they should be also in agreement with the neutrino oscillation data [31], and the lepton flavor violating (LFV) constraints [32]. In the SI framework, the non negligible contributions of the new DM annihilation channels $N_1 N_1 \rightarrow SS, VV, q\bar{q}$ could relax the bounds on these new couplings and make the parameters space (especially the range of the couplings $g_{i\alpha}$) much larger. The new DM-Higgs/dilaton interactions that allow the new DM annihilation channels will lead to a tree-level DM-nucleon scattering cross section, contrary to the non SI models where it is a pure one-loop effect. Consequently, this makes the effect of the requirement of both the direct detection (DD) constraints and the relic density, very important on the scalar sector within the SI models. For this reason, investigating these effects is the motivation of our work by considering the model [29] as an example. In the non-SI scotogenic model with fermionic DM [33], the neutrino mass smallness is achieved by imposing a mass degeneracy between the neutral inert CP-even and CP-odd scalars, since relatively large values for the $g_{i\alpha}$ couplings are dictated by the DM relic density. This implies that one of the scalar quartic couplings must be suppressed $\lambda_5 = \mathcal{O}(10^{-10})$. Nonetheless, this fine-tuning could be avoided by extending the model with a real singlet that is charged under a global Z_4/Z_2 symmetry [34]. Here, we will investigate the possibility of non-suppressed λ_5 value within the SI framework due to the existence of new DM annihilation channels ($N_1 N_1 \rightarrow SS, VV, q\bar{q}$).

The paper is organized as follows. Section II is devoted to describe the SI scotogenic ν -DM model, in addition to the EWSB description within the SI framework. In section III, the DM relic density is estimated via an explicit and exact calculation of the cross section of all channels. In addition, to impose the DD bounds, the DM nucleon cross section formula is given. In section IV, we perform a random scan for the model parameters space to probe all the possible correlation aspects between the scalar sector and the DM requirements. Our conclusions are given in section V.

II. THE SCALE INVARIANT SCOTOGENIC MODEL

Here, the SM is extended by one inert doublet scalar, $S \sim (1, 2, 1)$, three singlet Majorana fermions $N_i \sim (1, 1, 0)$, and one real neutral singlet scalar $\phi \sim (1, 1, 0)$ to assist the radiative EWSB. The model is assigned by a global Z_2 symmetry $\{S, N_i\} \rightarrow \{-S, -N_i\}$, where all other fields being Z_2 -even, in order to make the lightest Z_2 -odd field $N_1 \equiv N_{\text{DM}}$ stable,

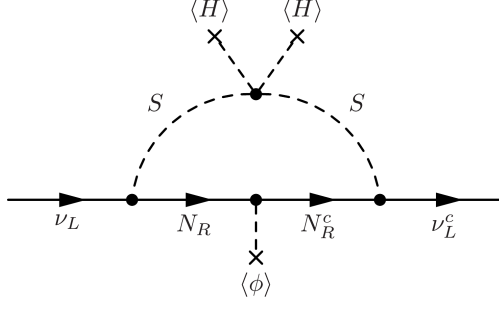


FIG. 1. The neutrino mass is generated in the SI-scotogenic model at one-loop level.

hence it plays the DM candidate role. The Lagrangian contains the following terms

$$\mathcal{L} \supset - \{g_{i\alpha} \overline{N}_i^c S^\dagger L_\alpha + \text{h.c.}\} - \frac{1}{2} y_i \phi \overline{N}_i^c N_i - V(H, S, \phi), \quad (1)$$

where the inert doublet can be presented as $S^T = (S^+, (S^0 + i A^0)/\sqrt{2}) \sim (1, 2, 1)$, L_β and $\ell_{\alpha R}$ the left-handed lepton doublet and right-handed leptons; the Greek letters label the SM flavors, $\alpha, \beta \in \{e, \mu, \tau\}$, $g_{i\alpha}$ and y_i are new Yukawa couplings. The most general SI scalar potential that obeys the Z_2 symmetry is given by

$$V_0(H, S, \phi) = \frac{1}{6} \lambda_H (|H|^2)^2 + \frac{\lambda_\phi}{24} \phi^2 + \frac{\lambda_S}{2} |S|^4 + \frac{\omega_1}{2} |H|^2 \phi^2 + \frac{\omega_2}{2} \phi^2 |S|^2 + \lambda_3 |H|^2 |S|^2 + \lambda_4 |H^\dagger S|^2 + \left\{ \frac{\lambda_5}{2} (H^\dagger S)^2 + \text{h.c.} \right\} \quad (2)$$

The first term in (1) and the last term in (2) are responsible for generating neutrino mass via the one-loop diagrams as illustrated in Fig. 1.

The neutrino mass matrix elements are given by [30]

$$m_{\alpha\beta}^{(\nu)} = \sum_i \frac{g_{i\alpha} g_{i\beta} M_i}{16\pi^2} \left[\frac{m_{S^0}^2}{m_{S^0}^2 - M_i^2} \log \frac{m_{S^0}^2}{M_i^2} - \frac{m_{A^0}^2}{m_{A^0}^2 - M_i^2} \log \frac{m_{A^0}^2}{M_i^2} \right]. \quad (3)$$

The neutrino mass matrix elements in (3) can be written as $m_{\alpha\beta}^{(\nu)} = \sum_i g_{i\alpha} g_{i\beta} \Lambda_i = (g^T \cdot A \cdot g)_{\alpha\beta}$, which permits us to write the new Yukawa couplings according to the Casas-Ibarra parameterization as [35]

$$g = D_{\sqrt{\Lambda^{-1}}} R D_{\sqrt{m_\nu}} U_\nu^T, \quad (4)$$

with $D_{\sqrt{\Lambda^{-1}}} = \text{diag}\{\Lambda_1^{-1/2}, \Lambda_2^{-1/2}, \Lambda_3^{-1/2}\}$, $D_{\sqrt{m_\nu}} = \text{diag}\{m_1^{1/2}, m_2^{1/2}, m_3^{1/2}\}$, R is an arbitrary 3×3 orthogonal matrix, m_i represents the neutrino mass eigenstates and U_ν is the Pontecorvo-Maki-Nakawaga-Sakata (PMNS) mixing matrix. These couplings are subject of the LFV bounds on the branching ratios of $\ell_\alpha \rightarrow \ell_\beta \gamma$ and $\ell_\alpha \rightarrow \ell_\beta \ell_\beta \ell_\beta$ [26].

In this model, the DM candidate could be fermionic (the lightest Majorana fermion, N_1) or a scalar (the lightest among S^0 and A^0). In the case of a scalar DM, the situation matches

the inert doublet model case [36], where the co-annihilation effect should be considered in order to have viable parameters space. For Majorana DM case, the Yukawa couplings $g_{i\alpha}$ values are constrained by the relic density, and therefore the neutrino mass smallness should be achieved by the $S^0 - A^0$ mass degeneracy, i.e., imposing a very small values for $\lambda_5 = \mathcal{O}(10^{-10})$.

After the EWSB, the CP-even neutral scalars acquire VEV's as

$$H \rightarrow \frac{v+h}{\sqrt{2}} \begin{pmatrix} 0 \\ 1 \end{pmatrix}, \quad \phi \rightarrow \frac{x+\phi}{\sqrt{2}}, \quad (5)$$

and hence give masses to all model fields, where we get two CP-even eigenstates

$$\begin{pmatrix} H \\ D \end{pmatrix} = \begin{pmatrix} c_\alpha & -s_\alpha \\ s_\alpha & c_\alpha \end{pmatrix} \begin{pmatrix} h \\ \phi \end{pmatrix}, \quad (6)$$

where H denotes the 125 GeV Higgs, D is the dilaton scalar and α is the Higgs-dilaton mixing angle, which is defined at tree-level as $s_\alpha = \sin \alpha = v/\sqrt{v^2 + x^2}$ and $c_\alpha = \cos \alpha = x/\sqrt{v^2 + x^2}$. In the SI approach, the EWSB is triggered by the the radiative corrections. Then, the one-loop effective potential in (2) can be expressed in the \overline{DR} scheme as

$$V^{1-\ell}(h, \phi) = \frac{\lambda_H + \delta\lambda_H}{24} h^4 + \frac{\lambda_\phi + \delta\lambda_\phi}{24} \phi^4 + \frac{\omega + \delta\omega}{4} h^2 \phi^2 + \frac{1}{64\pi^2} \sum_i n_i m_i^4(h, \phi) \left[\log \frac{m_i^2(h, \phi)}{\Lambda^2} - \frac{3}{2} \right], \quad (7)$$

where $\delta\lambda_H, \delta\lambda_\phi, \delta\omega$ are counter-terms, n_i and $m_i^2(h, \phi)$ are the field multiplicity and field dependant masses, respectively. Here $\Lambda = m_h = 125.18$ GeV is the renormalization scale and m_h is the measured Higgs mass. Here, we choose the counter-terms $\delta\lambda_H, \delta\lambda_\phi$ and $\delta\omega$, where the minimum $\{h = v, \phi = x\}$ is still the vacuum at one-loop; and the Higgs mass at one-loop must correspond to the measured value. The field dependent masses for the gauge bosons and fermions are the same as in the SM. The field dependent masses of the Goldstone and the Majorana singlets are $m_\chi^2 = \frac{1}{6}\lambda_H h^2 + \frac{1}{2}\omega\phi^2$ and $M_i^2 = y_i^2\phi^2$, respectively. The Higgs-dilation eigenmasses are the eigenvalues of the matrix whose elements are $m_{hh}^2 = \frac{1}{2}\lambda_H h^2 + \frac{1}{2}\omega\phi^2$, $m_{\phi\phi}^2 = \frac{1}{2}\lambda_\phi\phi^2 + \frac{1}{2}\omega h^2$ and $m_{h\phi}^2 = \omega h\phi$, and the inert field dependant masses are given by $m_{S^\pm}^2 = \frac{1}{2}\omega_2\phi^2 + \frac{1}{2}\lambda_3 h^2$, $m_{S^0, A^0}^2 = m_{S^\pm}^2 + \frac{1}{2}(\lambda_4 \pm \lambda_5)h^2$.

Since the dilaton acquires mass via radiative effects, then its mass squared should be positive $m_D^2 > 0$, which is basically guaranteed by the vacuum stability conditions. The vacuum stability could be ensured by imposing the coefficients of the term $\varphi^4 \log \varphi$ to be positive rather than the coefficients of the term φ^4 , where φ refers to any direction in the $h - \phi$ plan. These conditions are translated into

$$\begin{aligned} -12y_t^4 + \frac{9}{4}g_2^4 + \frac{3}{4}g_1^4 + \frac{4}{3}\lambda_H^2 + \frac{4}{3}\omega_1^2 + 2\lambda_3^2 + (\lambda_3 + \lambda_4 + \lambda_5)^2 + (\lambda_3 + \lambda_4 - \lambda_5)^2 &> 0, \\ \lambda_\phi^2 + 4\omega_1^2 + 4\omega_2^2 - 8(y_1^4 + y_2^4 + y_3^4) &> 0. \end{aligned} \quad (8)$$

As mentioned earlier, the EWSB is triggered by the radiative corrections, where the Higgs/dilaton sector has a similar structure for all the SI ν -DM models. However, there may be some few differences due to the nature and multiplicity of the new fields. Indeed, the new model couplings are not fully free and are severely constrained by many conditions such as the measured Higgs mass and the vacuum stability. Since the dilaton squared mass is purely radiative, we try to quantify the radiative effects by the values of both of the dilaton squared mass and the one-loop correction to Higgs/dilaton mixing

$$\Delta_{s_\alpha} = \frac{(s_\alpha)_{1-loop} - (s_\alpha)_{tree-level}}{(s_\alpha)_{tree-level}}. \quad (9)$$

These two quantities, in addition to the singlet VEV controls the new contribution of the DM annihilation via the interactions with the Higgs/dilaton, i.e., via the channels $N_1 N_1 \rightarrow h_i h_k, VV, q\bar{q}$ with $h_i = H, D$.

One has to mention that for other regions of space parameters, the light CP-even could match the SM-like Higgs, where the Higgs mass is generated fully radiative [37]. In this setup, the radiative effects push simultaneously the light CP-even mass to match the measured Higgs mass; and the scalar mixing to be in agreement with the Higgs signal strength measurements at the LHC [38]. In addition, this scenario is in agreement with all the previously mentioned constraints [37].

III. DARK MATTER

In this section, we discuss the relic density estimation approach and give the exact cross section formulas for the different annihilation channels. Then, we give the DM-nucleon scattering cross section that is subject of DD experiments.

DM Relic Density: the DM candidate is the lightest Majorana fermion (N_1), where there are many possible annihilation channels, that can be classify into two categories according to the DM interactions: (1) the annihilation via the new Yukawa interactions ($g_{i\alpha}$), i.e., into $N_1 N_1 \rightarrow \ell_\alpha \ell_\beta, \nu_\alpha \bar{\nu}_\beta$; and (2) the annihilation via the interactions with the Higgs/dilaton, i.e., $N_1 N_1 \rightarrow h_i h_k, VV, q\bar{q}$, where $S_i = H, D$ and $V = W, Z$. Clearly, for suppressed Higgs-dilaton mixing s_α , the situation matches the non SI models, i.e., the DM annihilation must fully achieved via the new Yukawa interactions. In the opposite case, the DM annihilation could be dominated by all channels (or simply by just one channel) that are mediated by the Higgs/dilaton. This depends on the DM mass M_1 , dilaton mass and the Higgs-dilaton mixing s_α .

In what follows, we show how could the DM relic density be estimated at the freeze-out temperature [39]. When the temperature of the Universe drops below the DM mass,

the DM decouples from the thermal bath and then preserves the DM particles number. In other words, after the freeze-out the ratio n_{DM}/n_s remains constant during the Universe expansion, where n_{DM} and n_s are the DM number and entropy densities, respectively. The estimated relic density must match the Planck observation [40]

$$\Omega_{DM}h^2 = 0.120 \pm 0.001, \quad (10)$$

where h is the reduced Hubble constant and Ω_{DM} denotes the DM energy density scaled by the critical density. Up to a very good approximation, the cold DM relic abundance of the WIMP scenario is given by [39]

$$\Omega_{N_1}h^2 \simeq \frac{(1.07 \times 10^9)x_F}{\sqrt{g_*}M_{pl}(\text{GeV}) \langle \sigma(N_1 N_1)v_r \rangle}, \quad (11)$$

where $x_F = M_1/T_F$ represents the freeze-out temperature, that can be determined iteratively from the equation

$$x_F = \log \left(\sqrt{\frac{45}{8}} \frac{M_1 M_{pl} \langle \sigma(N_1 N_1)v_r \rangle}{\pi^3 \sqrt{g_*} x_F} \right). \quad (12)$$

Here, v_r denotes the relative velocity, M_{pl} is the Plank mass, g_* counts the effective degrees of freedom of the relativistic fields in equilibrium, and

$$\langle \sigma(N_1 N_1)v_r \rangle = \sum_X \langle \sigma(N_1 N_1 \rightarrow X)v_r \rangle = \sum_X \int_{4M_1^2}^{\infty} ds \sigma_{N_1 N_1 \rightarrow X}(s) \frac{(s - 4M_1^2)}{8TM_1^4 K_2^2\left(\frac{M_1}{T}\right)} \sqrt{s} K_1\left(\frac{\sqrt{s}}{T}\right), \quad (13)$$

represents the total thermally averaged annihilation cross section. We have s is the Mandelstam variable, $K_{1,2}$ are the modified Bessel functions and $\sigma_{N_1 N_1 \rightarrow X}(s)$ is the partial annihilation cross due to the channel $N_1 N_1 \rightarrow X$, at the CM energy \sqrt{s} , where the possible channels are shown in Fig. 2.

We provide here the exact formulas for the partial annihilation cross sections. For the channels $N_1 N_1 \rightarrow \ell_\alpha \ell_\beta, \nu_\alpha \bar{\nu}_\beta$, we have [34, 41]

$$\begin{aligned} \sigma v_r &= \frac{1}{32\pi s^2} \sum_{\alpha, \beta} \sum_{X, Y} |\eta_X \eta_Y g_{1\alpha} g_{1\beta}^*|^2 \lambda(s, m_\alpha^2, m_\beta^2) \left\{ \mathcal{R}(Q_X, Q_Y, T_+, T_-, B) + \right. \\ &\quad \left. - \frac{M_1^2(s - m_\alpha^2 - m_\beta^2)}{B(Q_X + Q_Y)} \log \left| \frac{(Q_X + B)(Q_Y + B)}{(Q_X - B)(Q_Y - B)} \right| \right\}, \quad (14) \\ Q_X &= \frac{1}{2}(s + 2m_X^2 - 2M_1^2 - m_\alpha^2 - m_\beta^2), \quad T_\pm = \frac{1}{2}(s \pm m_\alpha^2 \mp m_\beta^2), \\ B &= \frac{1}{2s} \lambda(s, m_\alpha^2, m_\beta^2) \lambda(s, M_1^2, M_1^2), \quad \lambda(x, y, z) = \sqrt{(x - y - z)^2 - 4yz}, \\ \mathcal{R}(r, t, w, q, \eta) &= 2 - \frac{(t - w)(t - q)}{\eta(t - r)} \log \left| \frac{t + \eta}{t - \eta} \right| - \frac{(r - w)(r - q)}{\eta(r - t)} \log \left| \frac{r + \eta}{r - \eta} \right|. \end{aligned}$$

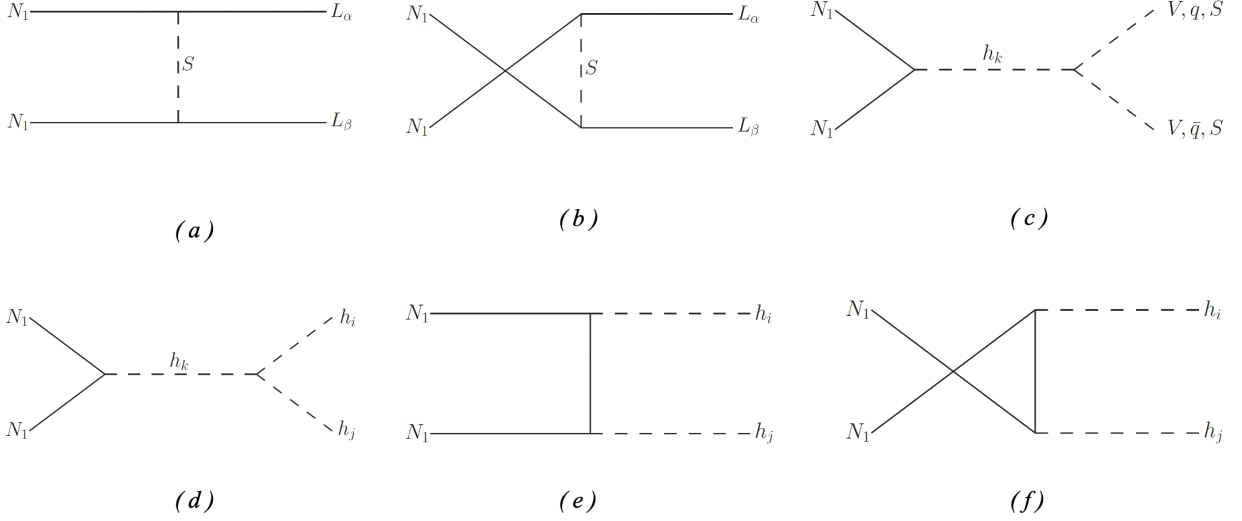


FIG. 2. Different DM annihilation channels in the SI-scotogenic model. The cross section in (14) is estimated based on the diagrams (a) and (b), while diagram (c) yields the cross section of the SM channels in (15). The Higgs/dilaton annihilation cross section in (16) is computed using the diagrams (d), (e) and (f).

For the channel $N_1 N_1 \rightarrow \ell_\alpha \ell_\beta$, we have: $m_\alpha = m_{\ell_\alpha}$, $m_\beta = m_{\ell_\beta}$, $\eta_{S^\pm} = i$ and $\{X, Y\} = \{S^\pm, S^\pm\}$. While, for the channel $N_1 N_1 \rightarrow \nu_\alpha \bar{\nu}_\beta$, we have: $m_\alpha = m_\beta = 0$, $\{X, Y\} = \{S^0, S^0\}, \{S^0, A^0\}, \{A^0, A^0\}$ and $\eta_{S^0} = \frac{i}{\sqrt{2}}$, $\eta_{A^0} = \frac{1}{\sqrt{2}}$.

For the channels that are mediated by the Higgs/dilaton ($N_1 N_1 \rightarrow X \bar{X}$, $X = W, Z, b, t$), one can write the cross section as [29]

$$\sigma(N_1 N_1 \rightarrow X \bar{X}) v_r = 8\sqrt{s} s_\alpha^2 c_\alpha^2 y_1^2 \left| \frac{1}{s - m_H^2 + im_H \Gamma_H} - \frac{1}{s - m_D^2 + im_D \Gamma_D} \right|^2 \Gamma_{H \rightarrow X \bar{X}}(m_H \rightarrow \sqrt{s}), \quad (15)$$

where $\Gamma_{H \rightarrow X \bar{X}}(m_H \rightarrow \sqrt{s})$ is the total SM Higgs decay width with the Higgs mass replaced by $m_H \rightarrow \sqrt{s}$. Here, $\Gamma_{H, D}$ are the Higgs and dilaton total decay widths, respectively. For simplicity, we take in our numerical scan $\Gamma_H \simeq \Gamma_h^{SM}$ and $\Gamma_D \simeq 0$. For the annihilation into Higgs/dilaton, we have the exact cross section formula at CM energy \sqrt{s} given by

$$\sigma(N_1 N_1 \rightarrow h_i h_j) v_r = \frac{1}{8\pi s} \left\{ R + \frac{W}{2B} \log \left| \frac{A - B}{A + B} \right| + \frac{Z}{A^2 - B^2} \right\}, \quad (16)$$

with $h_i = H, D$ and

$$\begin{aligned}
R &= \frac{1}{4}y_1^2(s - M_1^2)|Q|^2, \quad W = \frac{1 + \delta_{ij}}{2}q_i q_j y_1^3(s - M_1^2)M_1 \left(\Re(Q) + \frac{\delta_{ij}q_i q_j y_1 M_1}{(m_{h_i}^2 + m_{h_j}^2 - s)} \right), \\
Z &= \frac{1 + \delta_{ij}}{4}q_i^2 q_j^2 y_1^4 M_1^2 (s - M_1^2), \quad Q = \frac{-s_h \lambda_{Hij}}{s - m_H^2 + i m_H \Gamma_H} + \frac{c_h \lambda_{ijD}}{s - m_D^2 + i m_D \Gamma_D}, \\
A &= \frac{1}{2}(s - m_{h_i}^2 - m_{h_j}^2), \quad B = \frac{1}{2s} \lambda(s, M_1^2, M_1^2) \lambda(s, m_{h_i}^2, m_{h_j}^2),
\end{aligned}$$

where λ_{ijk} are the Higgs/dilaton triple couplings and $\{q_H = -s_\alpha, q_D = c_\alpha\}$.

DM Direct Detection: in the SI ν -DM models, the sensitivity to the direct-detection experiments could be due to the interactions between the DM and quarks via the mediation of the Higgs/dilaton. The effective low-energy Lagrangian of this interaction can be written as

$$\mathcal{L}_{N_1-q}^{(eff)} = -\frac{1}{2}s_\alpha c_\alpha y_q y_1 \left[\frac{1}{m_H^2} - \frac{1}{m_D^2} \right] \bar{q} q \bar{N}_1^c N_1, \quad (17)$$

where y_q is the light quark Yukawa coupling. Consequently, the effective nucleon-DM interaction can be written as

$$\mathcal{L}_{N_1-\mathcal{N}}^{(eff)} = \frac{s_\alpha c_\alpha (m_{\mathcal{N}} - \frac{7}{9}m_{\mathcal{B}})M_1}{x v} \left[\frac{1}{m_h^2} - \frac{1}{m_D^2} \right] \bar{\mathcal{N}} \mathcal{N} \bar{N}_1^c N_1, \quad (18)$$

where $m_{\mathcal{N}}$ is the nucleon mass and $m_{\mathcal{B}}$ the baryon mass in the chiral limit [42]. This leads to the nucleon-DM spin-independent elastic cross section in the chiral limit [29]

$$\sigma_{\text{det}} = \frac{c_\alpha^2 s_\alpha^2 m_{\mathcal{N}}^2 (m_{\mathcal{N}} - \frac{7}{9}m_{\mathcal{B}})^2 M_1^4}{\pi v^2 x^2 (M_1 + m_{\mathcal{B}})^2} \left[\frac{1}{m_h^2} - \frac{1}{m_D^2} \right]^2. \quad (19)$$

In what follows, we will consider the recent upper bound reported by Xenon 1T experiment [43]. In addition, we compare our results with the projected sensitivities for the future proposed experiments: PandaX-4t [44], LUX-Zeplin [45], XENONnT with 20 ton-yr exposure [46] and DARWIN [47].

IV. NUMERICAL RESULTS AND DISCUSSION

This model is subject to many theoretical and experimental constraints. Here, we will be interested in all phenomenological and experimental aspects of the Higgs/dilaton interactions and their correlation with DM relic density and DD, which may imply some constraints on the neutrino mass and the LFV processes. Then, in our numerical scan, we consider the following constraints: perturbativity, perturbative unitarity, the different Higgs decay channels (di-photon, invisible and undetermined), the electroweak precision tests, LEP negative

searches for light scalar (in our case, it applies to the cross section of $e^-e^+ \rightarrow ZD$), and the Higgs signal strength at the LHC $\mu_{\text{tot}} \geq 0.89$ at 95% CL [38]. The latter constraint (Higgs signal strength at the LHC [38]) can be expressed as $\mu_{\text{tot}} = c_\alpha^2 \times (1 - \mathcal{B}_{BSM}) \geq 0.89$, with c_α being the Higgs/dilaton mixing angle and \mathcal{B}_{BSM} is the branching ratio of any non-SM Higgs decay channel (could be the invisible channel like $H \rightarrow N_1N_1$ or/and an undermined channel like $H \rightarrow DD$), which are constrained as $\mathcal{B}_{BSM} \leq 0.47$ [48]. For a given value of \mathcal{B}_{BSM} , the condition $\mu_{\text{tot}} \geq 0.89$ can be translated at tree-level into a direct constraint on the singlet VEV value as: $x > 700.36$ GeV, 600 GeV, 480 GeV, 335 GeV, 233 GeV for $\mathcal{B}_{BSM} = 0, 0.038, 0.11, 0.27, 0.469$, respectively. However, one has to mention that in the SI models \mathcal{B}_{BSM} is likely to take values much smaller than the experimental bound due to the facts that the Higgs invisible decay branching ratio is s_α^2 proportional, and the triple coupling λ_{HDD} is suppressed since it has only a pure one-loop contribution. Here, we consider the input parameters ranges

$$\begin{aligned} 113.5 \text{ GeV} < m_{S^\pm} < 1 \text{ TeV}, \quad 10 \text{ GeV} < m_{S^0, A^0} < 1 \text{ TeV}, \quad 6 \text{ GeV} < M_1 < 1 \text{ TeV}, \\ 1 \text{ GeV} < m_D < 100 \text{ GeV}, \quad y_i^2, |\lambda_i| |g_{i\alpha}|^2 < 4\pi, \end{aligned} \quad (20)$$

where λ_i denotes all the couplings in (2). In the absence of BSM decay channels for the Higgs, the constraints $\mu_{\text{tot}} \geq 0.89$ implies that the singlet VEV is larger than $x > 700.36$ GeV, i.e., $x^2/(v^2 + x^2) \geq 0.89$. However, by considering the radiative correction in the mixing estimation, the singlet VEV could smaller as $x \geq \text{GeV}$. This is understood from the fact that the radiative corrections could be large so that the dilaton mass, which is a pure radiative effect, could reach values as $m_D \sim 100$ GeV, and the ratio Δ_{s_α} in (9) lies between $-1500\% < \Delta_{s_\alpha} < 1500\%$. This means that the scalar mixing could be dominated by the radiative corrections, and hence in our analysis, we will consider the one-loop value of the mixing s_α .

The existence of the Higgs/dilaton coupling to the Majorana DM candidate, N_1 in the SI models, leads to an addition contribution to the DM annihilation cross section via the channels $N_1N_1 \rightarrow h_i h_k, VV, q\bar{q}$, with h_i denotes the Higgs/dilaton and V denotes the gauge bosons. This new contribution could be either small or dominant depending on the parameters m_D, M_1 and the mixing $\sin \alpha$. Therefore, such a non-negligible new contribution makes the contribution of the channels $N_1N_1 \rightarrow \ell_\alpha \ell_\beta, \nu_\alpha \bar{\nu}_\beta$ smaller with respect to the non SI extended models. In other words, larger (smaller) contribution of the Higgs/dilaton mediated DM annihilation channels leads to smaller (larger) contribution of the channels $N_1N_1 \rightarrow \ell_\alpha \ell_\beta, \nu_\alpha \bar{\nu}_\beta$, and therefore smaller (larger) values of the new Yukawa couplings $g_{i\alpha}$, i.e., more precisely the combination $\sum_{\alpha, \beta} |g_{1\alpha} g_{1\beta}^*|^2$. Then, it would useful to define the ratio

$$\mathcal{R}_f = \frac{\langle \sigma(N_1N_1 \rightarrow f)v_r \rangle}{\langle \sigma(N_1N_1)v_r \rangle}, \quad (21)$$

that represents the contribution of the channel $N_1 N_1 \rightarrow f$ to the total thermally averaged cross section at the freeze-out. Clearly, we have $\sum_X \mathcal{R}_f = 1$, however, we will be interested in the two ratios: $\mathcal{R}_{LL} = \sum_{\alpha,\beta} (\mathcal{R}_{\ell_\alpha \ell_\beta} + \mathcal{R}_{\nu_\alpha \bar{\nu}_\beta})$ and $\mathcal{R}_{hh} = \sum_{h_i, k=H,D} \mathcal{R}_{h_i h_k}$ that represent the relative contributions of the channels $N_1 N_1 \rightarrow \ell_\alpha \ell_\beta, \nu_\alpha \bar{\nu}_\beta$ and $N_1 N_1 \rightarrow h_i h_k$ to the annihilation cross section, respectively. Clearly the ratio \mathcal{R}_{LL} is proportional to the combination $\sum_{\alpha,\beta} |g_{1\alpha} g_{1\beta}^*|^2$ in the limit of degenerate charged lepton masses. For a given DM mass value M_1 , let's call $\langle \sigma_0 v_r \rangle = \langle \sigma(N_1 N_1) v_r \rangle$ the correct cross section value at the freeze-out that matches the observed relic density (10). Then, the cross section of all Higgs/dilaton mediated channels $\sum_f \langle \sigma(N_1 N_1 \rightarrow f) v_r \rangle$ ($f = h_i h_k, VV, q\bar{q}$) at the freeze-out should be smaller than $\langle \sigma_0 v_r \rangle$. Therefore, the condition $\sum_f \langle \sigma(N_1 N_1 \rightarrow f) v_r \rangle \geq \langle \sigma_0 v_r \rangle$ leads to a value for the relic density that is smaller than the measured value and can not be compensated by the channels $N_1 N_1 \rightarrow \ell_\alpha \ell_\beta, \nu_\alpha \bar{\nu}_\beta$. This condition, together with the spin-independent DM DD cross section (19) would eliminate a significant part of the parameters space of any SI model that addresses the neutrino mass and Majorana DM together.

In order to investigate the impact of these constraints, we perform a random scan over the input parameters ranges in (20), while taking into account the theoretical and experimental constraints mentioned earlier. Since the case where the DM annihilation does fully occur via the channel $N_1 N_1 \rightarrow \ell_\alpha \ell_\beta, \nu_\alpha \bar{\nu}_\beta$, is phenomenologically identical the minimal scotogenic model [33], we will focus on the regions of the parameters space where the contributions of the other channels $N_1 N_1 \rightarrow h_i h_k, VV, q\bar{q}$ are not vanishing. We consider 4000 benchmark points (BPs) that fulfill all the conditions mentioned above and shown in Fig. 3-top and Fig. 3-bottom, the possible values of $\{m_D - s_\alpha^2\}$ for different values of the DM mass M_1 , singlet VEV x , and the ratios \mathcal{R}_{LL} and \mathcal{R}_{hh} .

One has to mention that for a significant part the BPs (not considered in Fig. 3) that pass all the requirements, the DM annihilation is almost fully achieved via $N_1 N_1 \rightarrow \ell_\alpha \ell_\beta, \nu_\alpha \bar{\nu}_\beta$. From Fig. 3, one can learn many conclusions, for instance, light dilaton ($m_D < 25$ GeV) and large mixing ($s_\alpha > 0.1$) correspond to light DM and large singlet VEV. In this region the DM annihilation is dominated by light quarks, charged leptons and/or neutrinos. Most of the BPs with large dilaton mass ($m_D > m_H/2$) and small mixing ($s_\alpha < 0.1$) correspond to light singlet VEV ($x < 900$ GeV) and heavy DM ($M_1 \sim O(100$ GeV)). In this region, the DM annihilation could be dominated either by $N_1 N_1 \rightarrow \ell_\alpha \ell_\beta, \nu_\alpha \bar{\nu}_\beta$ or by the channel $N_1 N_1 \rightarrow S_i S_k$. For the region of large mixing ($s_\alpha > 0.3$) the DM annihilation channel $N_1 N_1 \rightarrow S_i S_k$ is always suppressed despite the dilaton mass, while the channel $N_1 N_1 \rightarrow \ell_\alpha \ell_\beta, \nu_\alpha \bar{\nu}_\beta$ is dominated for part of the BPs. It should be stated that for the region of small mixing ($s_\alpha < 0.01$) and small dilaton mass ($m_D < m_H/2$), there exist possible viable BPs but with less population. For these BPs, the DM annihilation is fully achieved via the channel dominated either by $N_1 N_1 \rightarrow \ell_\alpha \ell_\beta, \nu_\alpha \bar{\nu}_\beta$, that matches phenomenologically the

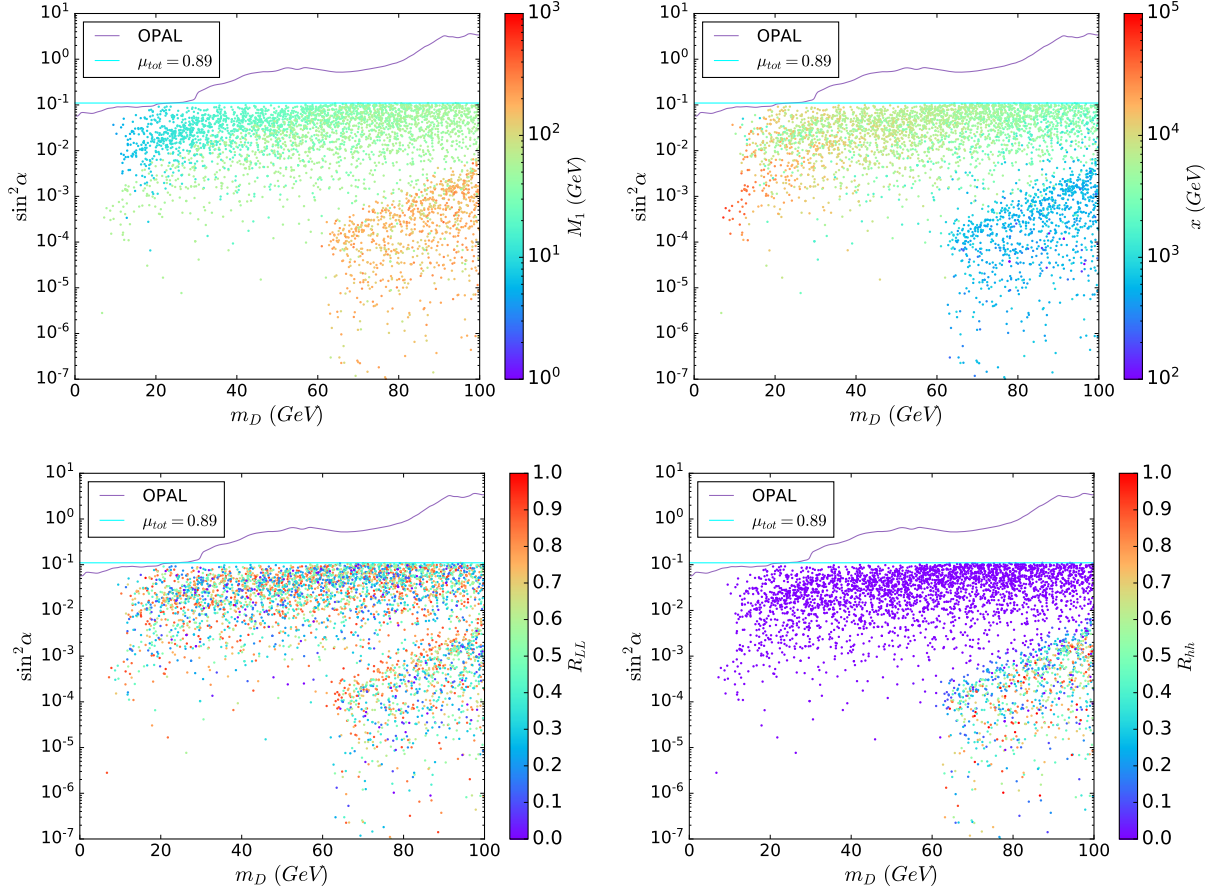


FIG. 3. The dilaton mass versus the Higgs/dilaton mixing, where the palette shows the DM mass (up-right), the singlet VEV (up-left), the ratio \mathcal{R}_{LL} (bottom-right) and the ratio \mathcal{R}_{hh} (bottom-left). The DM requirements of relic density and direct detection bounds, in addition to the LEP (OPAL) bound on $e^-e^+ \rightarrow Z^*D$ are already considered.

non-SI (minimal) scotogenic model.

For a complete picture, we show in Fig. 4 the DM-nucleon spin-independent cross section versus the DM mass, while the palette represents the dilaton mass (left) and the scalar mixing (right).

Clearly, from Fig. 4 a significant part of the BPs are within the reach of future DD experiments such as PandaX-4t [44], LUX-Zeplin [45] and XENONnT [46], while few of them (either with suppressed mixing $|s_\alpha| < 10^{-3}$ or with light DM $M_1 < 10$ GeV) could not be detected since they are below the neutrino floor. For viable DM with mass values larger than $M_1 > 100$ GeV, the scalar mixing should be $|s_\alpha| \lesssim 0.03$ and the dilaton mass $m_D \gtrsim 70$ GeV. However, for $20 \text{ GeV} \leq M_1 \leq 60$ GeV, the scalar mixing is almost maximal $|s_\alpha| \sim 0.1$. The population distribution around $M_1 \sim m_H/2$ implies that the analysis in this region requires a careful treatment.

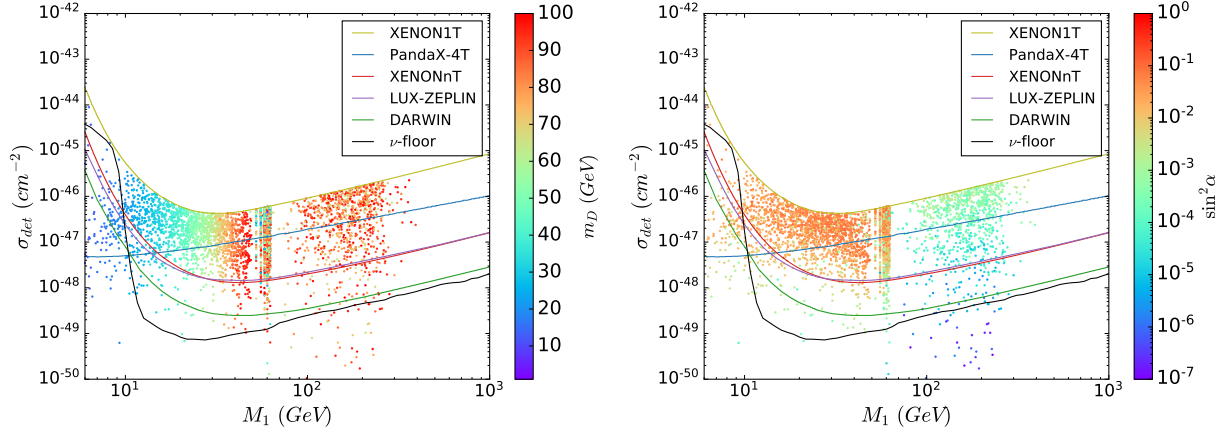


FIG. 4. The DM direct detection cross section versus the DM mass is presented, where the recent bound of Xenon 1T experiment is shown [43]. the palette illustrates the dilaton mass (left) and the scalar mixing (right). In addition, we show the projected sensitivities for the future experiments: PandaX-4t [44], LUX-Zeplin [45], XENONnT with 20 ton-yr exposure [46] and DARWIN [47]. The black line represents the neutrino floor, where any of the DM detection via nucleon scattering is not possible.

The contribution of the channel $N_1 N_1 \rightarrow \ell_\alpha \ell_\beta, \nu_\alpha \bar{\nu}_\beta$ to the total DM annihilation may take any value from almost 0% to almost 100%, for the whole range of both dilation and DM masses. This implies a relative freedom in the new Yukawa couplings range ($g_{i\alpha}$) contrary to the case of non SI version where the new Yukawa coupling values are strictly dictated by the relic density. In order to illustrate this point, we show in Fig. 5-left the correlation between the ratios \mathcal{R}_{LL} and \mathcal{R}_{hh} and the quartic coupling λ_5 for the 4000 BPs used previously in Fig. 3. In order to show the explicit dependence of the scalar coupling λ_5 on the ratio \mathcal{R}_{LL} , we consider the BPs shown in Table. I among the 4000 points, which all correspond to a maximal $\mathcal{R}_{LL} \sim 1$.

Next, we assume that one can make the ratio \mathcal{R}_{LL} smaller by re-scaling the new Yukawa couplings $g_{i\alpha}$ to smaller values, while keeping the inert parameters ($M_i, x, \omega_2, \lambda_3$ and λ_4) constant. In this case, both neutrino mass matrix elements in (3) and the DM relic density can be kept in agreement with the data, only by allowing λ_5 to have larger values, by and tuning the radiative effects (dilaton mass and scalar mixing), respectively. Therefore, the dependence of the ratio \mathcal{R}_{LL} on λ_5 is shown in Fig. 5-right where the palette shows the couplings combination $\sum_{i,k} |g_{1,i} g_{1k}^*|^2$ that is proportional to the cross section of $N_1 N_1 \rightarrow \ell_\alpha \ell_\beta, \nu_\alpha \bar{\nu}_\beta$ in the massless charged leptons limit.

For the 4000 BPs considered in Fig. 5-left, the scalar coupling can be relaxed up to $\lambda_5 \sim 10^{-5}$ contrary to the non-SI case where $\lambda_5 \sim 10^{-10}$. From Fig. 5-right, one notices that

	BP1	BP2	BP3	BP4
m_D (GeV)	16.25	89.47	60.27	93.42
s_α	0.22685	0.01467	-0.01905	-0.07311
x (GeV)	856.34	393.7	1115.3	1657.4
m_{S^\pm} (GeV)	257.6	308.12	445.60	667.25
\bar{m} (GeV)	250.6	409.37	428.21	750.46
M_1 (GeV)	6.31	81.94	175.20	467.81
M_2 (GeV)	6.67	88.69	186.59	532.69
M_3 (GeV)	7.34	96.14	220.03	602.23
x_f	21.94	24.27	24.89	25.89
$\sum_{i,k} g_{1,i} g_{1k}^* ^2$	2.48×10^{-5}	3.51×10^{-3}	1.31×10^{-2}	7.02×10^{-2}
\mathcal{R}_{LL}	0.9918	0.98063	0.96442	0.95498
\mathcal{R}_{hh}	1.21×10^{-33}	0.01857	0.0355	0.0450
λ_5	5.6196×10^{-7}	1.1265×10^{-8}	2.7543×10^{-9}	-1.8715×10^{-9}

TABLE I. The benchmark points used in Fig. 5-bottom. Here, we have $\bar{m}^2 = \frac{1}{2}(m_{S^0}^2 + m_{A^0}^2)$, $x_f = M_1/T_f$ is freeze-out parameter, and the couplings combination $\sum_{i,k} |g_{1,i} g_{1k}^*|^2$ is proportional to the cross section of $N_1 N_1 \rightarrow \ell_\alpha \ell_\beta, \nu_\alpha \bar{\nu}_\beta$ in the limit of massless charged leptons.

by tuning the radiative effects (dilaton mass and scalar mixing), one can push the scalar coupling up to larger values as $\lambda_5 \sim 1$. Consequently, the new Yukawa couplings can be much small as shown by the palette in Fig. 5-right, i.e., $\lambda_5 \sim 1 \implies \sum_{i,k} |g_{1,i} g_{1k}^*|^2 \leq 10^{-4}$. This conclusion can be extrapolated into other models like the SI-KNT model [10], however, getting larger values for $\lambda_5 \sim 0.1 - 1$ in any SI model is not possible except for the case where the model new couplings and masses can be tuned without being in conflict with the above mentioned theoretical and experimental constraints.

The SI-scotogenic model with Majorana DM candidate has almost the same LHC predictions as the minimal scotogenic model [33]. For instance, a pair of charged scalars that are produced at the LHC ($pp \rightarrow S^\pm S^\mp$) leads to many distinguishable signatures such as $4\text{jets} + \cancel{E}_T$, $1\ell + 2\text{jets} + \cancel{E}_T$ and $2\ell + \cancel{E}_T$. Moreover, the process $pp \rightarrow S^\pm S^0, S^\pm A^0$ may lead to the signatures $1\ell + 2\text{jets} + \cancel{E}_T$ and $1\ell + \cancel{E}_T$. However, the process $pp \rightarrow S^0 S^0, A^0 A^0$ results the final states $\cancel{E}_T + \text{ISR}$ (mono-jet, mono- γ). In order to distinguish the SI-scotogenic model among its minimal version at colliders, one has to look for signatures that exit only in the SI-version like $pp \rightarrow N_1 N_1 \gamma(H), pp \rightarrow H \rightarrow DD \rightarrow 4b, 4\tau, 2b2\tau, 2b2\gamma$. As mentioned previously, the new Yukawa couplings $g_{i\alpha}$ can take small values, especially in the case where

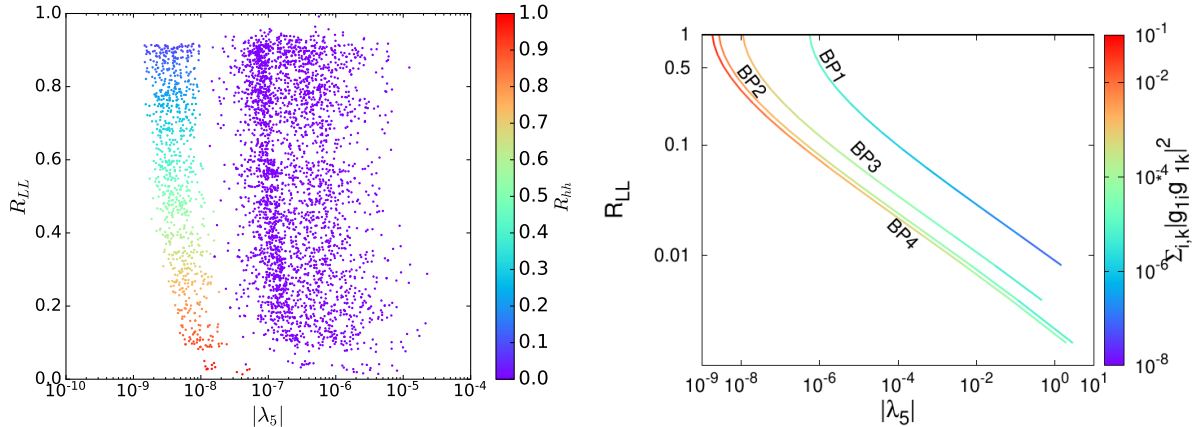


FIG. 5. Left: the ratio \mathcal{R}_{LL} versus the scalar coupling λ_5 for the 4000 BPs used previously in Fig. 3, where the palette shows the ratio \mathcal{R}_{hh} . Right: the dependence of the ratio \mathcal{R}_{LL} on the scalar coupling λ_5 for the BPs shown in Table. I, where both DM relic density and neutrino masses are kept in agreement with the data. The palette shows the couplings combination $\sum_{i,k} |g_{1,i} g_{1k}^*|^2$ that is proportional to the cross section of $N_1 N_1 \rightarrow \ell_\alpha \ell_\beta, \nu_\alpha \bar{\nu}_\beta$ in the limit of massless charged leptons.

$\mathcal{R}_{LL} \ll 1$, which basically makes the life-time of the charged scalar (S^\pm) longer and then, displaced vertices can be seen in $pp \rightarrow S^\pm S^\pm, S^\pm S^0, S^\pm A^0$ due to $S^\pm \rightarrow \ell^\pm N_1$.

V. CONCLUSION

In this work, we have considered the SI-scotogenic model that addresses neutrino oscillation data, DM nature and the EWSB, all together at the weak scale. In this model, the EWSB is triggered by radiative effects due to new fields and interactions in addition to the SM one. The DM candidate could be the lightest among the CP-even, CP-odd scalars or lightest Majorana singlet fermion, here we adopted a Majorana DM candidate. After discussing the EWSB we imposed different theoretical and experimental constraints like the vacuum stability, the electroweak precision tests, LEP negative searches for light scalars, the Higgs decays ($h \rightarrow \gamma\gamma$, invisible, undertermined), DM relic density and DM DD experiments. The DM relic density was estimated following [39], where the cross section of different annihilation channels was estimated exactly, including those of $N_1 N_1 \rightarrow \ell_\alpha \ell_\beta, \nu_\alpha \bar{\nu}_\beta$.

In the non SI (minimal scotogenic) version of the model, the DM annihilation occurs via the channel $N_1 N_1 \rightarrow \ell_\alpha \ell_\beta, \nu_\alpha \bar{\nu}_\beta$, which dictates the values of the new Yukawa couplings $g_{i\alpha}$ that relatively large. In addition, the neutrino mass smallness can be achieved by imposing the a mass degeneracy between the CP-even and the CP-odd scalars, which

means a suppressed value for the coupling $\lambda_5 = (m_{S^0}^2 - m_{A^0}^2)/v^2 \sim 10^{-10}$. Due to non negligible coupling for DM with the Higgs/dilaton, other DM annihilation channels such as $N_1 N_1 \rightarrow h_i h_k, VV, q\bar{q}$ are possible, and therefore the new Yukawa couplings $g_{i\alpha}$ could take smaller values with respect to the non-SI case. This means that Majorana DM is possible without a mass degeneracy between the CP-even and the CP-odd scalars.

By considering all the previous listed theoretical constraints, and focusing on benchmark points (BPs) that are different from non SI version, i.e., BPs with non negligible contributions of the channels $N_1 N_1 \rightarrow h_i h_k, VV, q\bar{q}$ to the total DM annihilation, we performed a numerical scan over the parameters space. We have found that the DM annihilation could be dominated by light quarks, charged leptons and/or neutrinos channels for light dilaton ($m_D < 25$ GeV), large mixing ($s_\alpha > 0.1$), light DM ($M_1 < 10$ GeV) and large singlet VEV ($x > 2$ TeV). Another interesting region for large dilaton mass ($m_D > m_H/2$), small mixing ($s_\alpha < 0.1$), small singlet VEV ($x < 900$ GeV) and heavy DM ($M_1 \sim O(100$ GeV)), where the DM annihilation could be dominated either by $N_1 N_1 \rightarrow \ell_\alpha \ell_\beta, \nu_\alpha \bar{\nu}_\beta$ or by the channel $N_1 N_1 \rightarrow HH, HD, DD$. We found also that the values of the scalar quartic coupling can be relaxed up to $\lambda_5 \sim 10^{-5}$ contrary to the non-SI case where $\lambda_5 \sim 10^{-10}$. By possible tuning of the radiative effects (in our model due to $M_i, x, \omega_2, \lambda_3$ and λ_4), the scalar coupling could be $\lambda_5 \sim 1$, which implies very small values for the new Yukawa couplings $\sum_{i,k} |g_{1,i} g_{1k}^*|^2 \leq 10^{-4}$. These regions are the most important regions where the SI extension of the scotogenic model (as well other models like the SI-KNT), in which the Majorana DM phenomenology is different than the non SI version. These regions are with a great interest and their phenomenology studies at colliders is ongoing in a future work [49].

Acknowledgements

This work is supported by the University of Sharjah via the following grants: *Probing the Majorana Neutrino Nature in Radiative Neutrino Mass Models at Current and Future Colliders* (No. 1802143057-P), *Extended Higgs Sectors at Colliders: Constraints & Predictions* (No. 21021430100) and *Hunting for New Physics at Colliders* (No. 21021430107). The authors thank S. Nasri for his valuable comments.

-
- [1] S. R. Coleman and E. J. Weinberg, Phys. Rev. D **7** (1973), 1888-1910
 - [2] M. Gell-Mann, P. Ramond, and R. Slansky, in Supergravity, edited by P. van Nieuwenhuizen and D. Z. Freedman (North-Holland, Amsterdam, 1979), p. 315; T. Yanagida, in Proceedings of the Workshop on the Unified Theory and the Baryon Number in the Universe, edited by

- O. Sawada and A. Sugamoto, KEK Report No. 79-18 (Tsukuba, Japan, 1979), p. 95; R. N. Mohapatra and G. Senjanovic, Phys. Rev. Lett. 44, 912 (1980). J. Schechter and J. W. F. Valle, Phys. Rev. D **22**, 2227 (1980). J. Schechter and J. W. F. Valle, Phys. Rev. D **25**, 774 (1982).
- [3] E. Ma, Phys. Rev. Lett. **81**, 1171 (1998) [[hep-ph/9805219](#)].
- [4] A. Zee, Phys. Lett. B **161** (1985), 141-145
- [5] A. Zee, Nucl. Phys. B **264**, 99 (1986).
- [6] K. S. Babu, Phys. Lett. B **203**, 132 (1988).
- [7] M. Aoki, S. Kanemura, T. Shindou and K. Yagyu, JHEP **07** (2010), 084 [erratum: JHEP **11** (2010), 049] [[arXiv:1005.5159](#)] [hep-ph].
- [8] G. Guo, X. G. He and G. N. Li, JHEP **10** (2012), 044 [[arXiv:1207.6308](#)] [hep-ph].
- [9] Y. Kajiyama, H. Okada and K. Yagyu, Nucl. Phys. B **874** (2013), 198-216 [[arXiv:1303.3463](#)] [hep-ph].
- [10] A. Ahriche, K. L. McDonald and S. Nasri, JHEP **02** (2016), 038 [[arXiv:1508.02607](#)] [hep-ph].
- [11] L. M. Krauss, S. Nasri and M. Trodden, Phys. Rev. D **67** (2003), 085002 [[arXiv:hep-ph/0210389](#)] [hep-ph].
- [12] M. Aoki, S. Kanemura and O. Seto, Phys. Rev. Lett. **102**, 051805 (2009) [[arXiv:0807.0361](#)] [hep-ph]; M. Aoki, S. Kanemura and O. Seto, Phys. Rev. D **80**, 033007 (2009) [[arXiv:0904.3829](#)] [hep-ph].
- [13] M. Gustafsson, J. M. No and M. A. Rivera, Phys. Rev. Lett. **110**, no. 21, 211802 (2013) Erratum: [Phys. Rev. Lett. **112**, no. 25, 259902 (2014)] [[arXiv:1212.4806](#)] [hep-ph].
- [14] H. Okada and K. Yagyu, Phys. Rev. D **93**, no. 1, 013004 (2016) [[arXiv:1508.01046](#)] [hep-ph]; L. G. Jin, R. Tang and F. Zhang, Phys. Lett. B **741**, 163 (2015) [[arXiv:1501.02020](#)] [hep-ph]; K. Cheung, T. Nomura and H. Okada, [arXiv:1610.04986](#) [hep-ph]; S. Baek, H. Okada and T. Toma, JCAP **1406**, 027 (2014) [[arXiv:1312.3761](#)] [hep-ph]; S. Kashiwase, H. Okada, Y. Orikasa and T. Toma, Int. J. Mod. Phys. A **31**, no. 20n21, 1650121 (2016) [[arXiv:1505.04665](#)] [hep-ph]; S. Kanemura, K. Nishiwaki, H. Okada, Y. Orikasa, S. C. Park and R. Watanabe, PTEP **2016**, no. 12, 123B04 (2016) [[arXiv:1512.09048](#)] [hep-ph]; S. Kanemura, O. Seto and T. Shimomura, Phys. Rev. D **84**, 016004 (2011). E. Ma, Phys. Rev. D **73**, 077301 (2006) [[hep-ph/0601225](#)].
- [15] A. Ahriche, C. S. Chen, K. L. McDonald and S. Nasri, Phys. Rev. D **90**, 015024 (2014) [[arXiv:1404.2696](#)] [hep-ph]. A. Ahriche, K. L. McDonald and S. Nasri, JHEP **1410**, 167 (2014) [[arXiv:1404.5917](#)] [hep-ph]. L. Megrelidze and Z. Tavartkiladze, Nucl. Phys. B **914**, 553 (2017) [[arXiv:1609.07344](#)] [hep-ph].
- [16] B. Dutta, S. Ghosh, I. Gogoladze and T. Li, Phys. Rev. D **98** (2018) no.5, 055028 [[arXiv:1805.01866](#)] [hep-ph].

- [17] K. Cheung, T. Nomura and H. Okada, Phys. Lett. B **768** (2017), 359-364 [[arXiv:1701.01080](#) [hep-ph]].
- [18] P. H. Gu, JHEP **04** (2017), 159 [[arXiv:1611.03256](#) [hep-ph]].
- [19] H. Hatanaka, K. Nishiwaki, H. Okada and Y. Orikasa, Nucl. Phys. B **894** (2015), 268-283 [[arXiv:1412.8664](#) [hep-ph]].
- [20] K. Nishiwaki, H. Okada and Y. Orikasa, Phys. Rev. D **92** (2015) no.9, 093013 [[arXiv:1507.02412](#) [hep-ph]].
- [21] A. Ahriche, K. L. McDonald, S. Nasri and T. Toma, Phys. Lett. B **746** (2015), 430-435 [[arXiv:1504.05755](#) [hep-ph]].
- [22] T. Nomura, H. Okada and N. Okada, Phys. Lett. B **762** (2016), 409-414 [[arXiv:1608.02694](#) [hep-ph]].
- [23] T. Nomura and H. Okada, Phys. Lett. B **755** (2016), 306-311 [[arXiv:1601.00386](#) [hep-ph]].
- [24] M. Aoki, S. Kanemura, K. Sakurai and H. Sugiyama, Phys. Lett. B **763**, 352 (2016) [[arXiv:1607.08548](#) [hep-ph]]. P. Fileviez Perez, T. Han, G. Y. Huang, T. Li and K. Wang, Phys. Rev. D **78**, 071301 (2008) [[arXiv:0803.3450](#) [hep-ph]]. C. S. Chen, C. Q. Geng, J. N. Ng and J. M. S. Wu, JHEP **0708**, 022 (2007) [[arXiv:0706.1964](#) [hep-ph]]. J. Kersten and A. Y. Smirnov, Phys. Rev. D **76**, 073005 (2007) [[arXiv:0705.3221](#) [hep-ph]]. A. Das and N. Okada, Phys. Rev. D **88**, 113001 (2013) [[arXiv:1207.3734](#) [hep-ph]]. D. Atwood, S. Bar-Shalom and A. Soni, Phys. Rev. D **76**, 033004 (2007) [[hep-ph/0701005](#)]. S. Antusch, E. Cazzato and O. Fischer, JHEP **1604**, 189 (2016) [[arXiv:1512.06035](#) [hep-ph]]. S. Antusch, E. Cazzato and O. Fischer, Int. J. Mod. Phys. A **32** (2017) no.14, 1750078 [[arXiv:1612.02728](#) [hep-ph]].
- [25] A. Ahriche, S. Nasri and R. Soualah, Phys. Rev. D **89**, no. 9, 095010 (2014) [[arXiv:1403.5694](#) [hep-ph]]. C. Guella, D. Cherigui, A. Ahriche, S. Nasri and R. Soualah, Phys. Rev. D **93**, no. 9, 095022 (2016) [[arXiv:1601.04342](#) [hep-ph]]. D. Cherigui, C. Guella, A. Ahriche and S. Nasri, Phys. Lett. B **762**, 225 (2016) [[arXiv:1605.03640](#) [hep-ph]]. S. Y. Ho and J. Tandean, Phys. Rev. D **89**, 114025 (2014) [[arXiv:1312.0931](#) [hep-ph]]. S. Kanemura, T. Nabeshima and H. Sugiyama, Phys. Rev. D **87**, no. 1, 015009 (2013) [[arXiv:1207.7061](#) [hep-ph]].
- [26] T. Toma and A. Vicente, JHEP **01** (2014), 160 [[arXiv:1312.2840](#) [hep-ph]]. M. Chekkal, A. Ahriche, A. B. Hammou and S. Nasri, Phys. Rev. D **95**, no. 9, 095025 (2017) [[arXiv:1702.04399](#) [hep-ph]].
- [27] Y. Cai, J. Herrero-García, M. A. Schmidt, A. Vicente and R. R. Volkas, [arXiv:1706.08524](#) [hep-ph]. S. M. Boucenna, S. Morisi and J. W. F. Valle, Adv. High Energy Phys. **2014**, 831598 (2014) [[arXiv:1404.3751](#) [hep-ph]];
- [28] R. Foot, A. Kobakhidze, K. L. McDonald and R. R. Volkas, Phys. Rev. D **76** 075014 (2007) [[arXiv:0706.1829](#) [hep-ph]]. H. Davoudiasl and I. M. Lewis, Phys. Rev. D **90**, no. 3, 033003

- (2014) [[arXiv:1404.6260](#) [hep-ph]]; M. Lindner, S. Schmidt and J. Smirnov, JHEP **1410**, 177 (2014) [[arXiv:1405.6204](#) [hep-ph]]; Z. Kang, Eur. Phys. J. C **75**, no. 10, 471 (2015) [[arXiv:1411.2773](#) [hep-ph]]; H. Okada and Y. Orikasa, [arXiv:1412.3616](#) [hep-ph]; J. Guo, Z. Kang, P. Ko and Y. Orikasa, Phys. Rev. D **91**, no. 11, 115017 (2015) [[arXiv:1502.00508](#) [hep-ph]]; P. Humbert, M. Lindner and J. Smirnov, JHEP **1506**, 035 (2015) [[arXiv:1503.03066](#) [hep-ph]]; P. Humbert, M. Lindner, S. Patra and J. Smirnov, JHEP **1509**, 064 (2015) [[arXiv:1505.07453](#) [hep-ph]]; Z. Kang, Phys. Lett. B **751**, 201 (2015) [[arXiv:1505.06554](#) [hep-ph]]; A. Karam and K. Tamvakis, Phys. Rev. D **92**, no. 7, 075010 (2015) [[arXiv:1508.03031](#) [hep-ph]]; H. Okada, Y. Orikasa and K. Yagyu, [arXiv:1510.00799](#) [hep-ph]; L. Alexander-Nunneley and A. Pilaftsis, JHEP **09** (2010), 021 [[arXiv:1006.5916](#) [hep-ph]].
- J. S. Lee and A. Pilaftsis, Phys. Rev. D **86** (2012), 035004 [[arXiv:1201.4891](#) [hep-ph]].
- [29] A. Ahriche, K. L. McDonald and S. Nasri, JHEP **06** (2016), 182 [[arXiv:1604.05569](#) [hep-ph]].
- [30] E. Ma, Phys. Rev. D **73** (2006), 077301 [[arXiv:hep-ph/0601225](#) [hep-ph]].
- [31] S. Fukuda *et al.* [Super-Kamiokande Collaboration], Phys. Rev. Lett. **86**, 5651 (2001) [[hep-ex/0103032](#)]. Q. R. Ahmad *et al.* [SNO Collaboration], Phys. Rev. Lett. **87**, 071301 (2001) [[nucl-ex/0106015](#)].
- [32] P. A. Zyla *et al.* (Particle Data Group), Prog. Theor. Exp. Phys. 2020, **083C01** (2020) and 2021 update.
- [33] A. Ahriche, A. Jueid and S. Nasri, Phys. Rev. D **97** (2018) no.9, 095012 [[arXiv:1710.03824](#) [hep-ph]]. A. Ahriche, A. Arhrib, A. Jueid, S. Nasri and A. de La Puente, Phys. Rev. D **101** (2020) no.3, 035038 [[arXiv:1811.00490](#) [hep-ph]].
- [34] A. Ahriche, A. Jueid and S. Nasri, Phys. Lett. B **814** (2021), 136077 [[arXiv:2007.05845](#) [hep-ph]].
- [35] J. A. Casas and A. Ibarra, Nucl. Phys. B **618** (2001), 171-204 [[arXiv:hep-ph/0103065](#) [hep-ph]].
- [36] S. Banerjee, F. Boudjema, N. Chakrabarty and H. Sun, [[arXiv:2101.02165](#) [hep-ph]]. S. Banerjee, F. Boudjema, N. Chakrabarty and H. Sun, [[arXiv:2101.02166](#) [hep-ph]]. S. Banerjee, F. Boudjema, N. Chakrabarty and H. Sun, [[arXiv:2101.02167](#) [hep-ph]]. S. Banerjee, F. Boudjema, N. Chakrabarty and H. Sun, [[arXiv:2101.02170](#) [hep-ph]].
- [37] A. Ahriche, “Scale invariant models without a light dilaton,” [[arXiv:2110.10301](#) [hep-ph]].
- [38] G. Aad *et al.* [ATLAS and CMS], JHEP **08** (2016), 045 [[arXiv:1606.02266](#) [hep-ex]]. G. Arcadi, A. Djouadi and M. Raidal, Phys. Rept. **842** (2020), 1-180 [[arXiv:1903.03616](#) [hep-ph]].
- [39] M. Srednicki, R. Watkins and K. A. Olive, Nucl. Phys. B **310**, 693 (1988) E. W. Kolb and M. S. Turner, Front. Phys. **69**, 1 (1990).

- [40] N. Aghanim *et al.* [Planck], *Astron. Astrophys.* **641**, A6 (2020) [[arXiv:1807.06209](#)] [astro-ph.CO].
- [41] I. Lalili, “*The Annihilation Cross Section in Majorana Dark Matter Models: Exact Estimation*”, Master thesis 2019, Jijel University, Algeria.
- [42] X. G. He, T. Li, X. Q. Li, J. Tandean and H. C. Tsai, *Phys. Rev. D* **79**, 023521 (2009) [[arXiv:0811.0658](#)] [hep-ph].
- [43] E. Aprile *et al.* [XENON], *Phys. Rev. Lett.* **121** (2018) no.11, 111302 [[arXiv:1805.12562?](#)] [astro-ph.CO].
- [44] H. Zhang *et al.* [PandaX], *Sci. China Phys. Mech. Astron.* **62** (2019) no.3, 31011 [[arXiv:1806.02229](#)] [physics.ins-det].
- [45] D. S. Akerib *et al.* [LUX-ZEPLIN], *Phys. Rev. D* **101** (2020) no.5, 052002 [[arXiv:1802.06039](#)] [astro-ph.IM].
- [46] E. Aprile *et al.* [XENON], *JCAP* **11** (2020), 031 [[arXiv:2007.08796](#)] [physics.ins-det].
- [47] J. Aalbers *et al.* [DARWIN], *JCAP* **11** (2016), 017 [[arXiv:1606.07001](#)] [astro-ph.IM].
- [48] G. Aad *et al.* [ATLAS], *Phys. Rev. D* **101**(2020), no.1, 012002 [[arXiv:1909.02845](#)] [hep-ex].
M. Aaboud *et al.* [ATLAS], *Phys. Rev. Lett.* **122** (2019) no.23, 231801 [[arXiv:1904.05105](#)] [hep-ex].
- [49] A. Ahriche and R. Soualah, *in progress*.